ADVANCES IN PORO-VASCULAR COMPOSITES: TOWARD NON-MECHANICAL SURFACE ROUGHNESS CONTROL

Russell C. Reid[1], James P. Thomas[2] and Marriner H. Merrill[3]

[1] American Society for Engineering Education – U.S. Naval Research Laboratory (ASEE-NRL)

[2,3] U.S. Naval Research Laboratory, 4555 Overlook Avenue SW, Washington, DC 20375-5343, USA

[1] Email: russell.reid.ctr@nrl.navy.mil
[2] Email: james.p.thomas@nrl.navy.mil
[3] Email: mariner.merrill@nrl.navy.mil

Keywords: multifunctional, electrowetting-on-dielectric, microfluidics, unmanned air vehicle

ABSTRACT

The U.S. Naval Research Laboratory (NRL) is developing poro-vascular composites (PVCs) with structural skin and active surface roughness control functionalities. This paper describes recent progress on PVC component design for liquid-phase control and the development of a new EWOD actuator for controlling liquid pressure via contact angles, which enables pore-exit menisci shape control with improved response and reversibility. Key design features for liquid control include: pore geometry and diameter uniformity, actuator substrate quality, and actuator substrate gap to pore radius ratio. Careful attention to these details has yielded pore-exit contact angle changes greater than 100 degrees in current PVC laboratory prototypes. Contact angle hysteresis, caused by liquid pinning inside the actuator, and pore meniscus instabilities under boundary-layer flow are two ongoing challenges to achieving stable and reversible surface roughness control for potential airfoil performance improvements.

1 INTRODUCTION

The U.S. Naval Research Laboratory is developing multifunctional poro-vascular composites (PVCs) as a structural skin with surface roughness control. PVCs are being fabricated using fiber-polymer laminates with internal vascular networks that are connected to mm-scale pore arrays on the surface. The internal channels are filled with a non-volatile liquid phase whose menisci shape and height are controlled at the pore exits using electrowetting-on-dielectric (EWOD) and volume-displacement pumping. The research has focused on multifunctional design, fabrication, and characterization of PVCs with optimized mechanical properties (that minimize pore and internal channel effects) and robust and repeatable liquid-phase sensing and control at the pore-exits. Controllable menisci configurations at the pore-exits (dome, flat, dimple; Figure 1) may be useful for creating a switchable "trip-strip" for initiating the laminar-turbulent transition on small unmanned air-vehicle (SUAV) airfoils or for SUAV steering using localized variations in airfoil drag that would minimize or eliminate the need for servo-flaps.

Achieving robust and repeatable (low-hysteresis) control of the liquid menisci at multiple sub-mm pore exits presents significant challenges. The pore geometry and surface wetting characteristics inside and around the pore must be tailored to achieve liquid pinning at the pore-exit and account for (slight) pore-to-pore dimensional variations. In SUAV airfoil applications, spatial variations in aerodynamic pressure during boundary-layer flows and structural deformations of the pores and channels can produce dynamic and spatial variations in the menisci shapes and heights. Mitigation of such effects requires sensing and control of the menisci shape and height. The full range of menisci states from dome to flat to dimple can be achieved by combining EWOD with displacement pumping. Multifunctional design is being used to size the pores, channels, EWOD liquid control reservoir, pump, and fluidic connections for proper operations under quasi-static conditions and for limiting/minimizing pore and channel (cut-out) effects on the laminate's structural stiffness and strength. Aerodynamic modeling and wind-tunnel experiments will be conducted in the future to determine pore shapes (e.g., circular, square), sizes, array

configurations, and locations on the airfoil for effective boundary-layer flow control leading to useful SUAV flight performance enhancements.

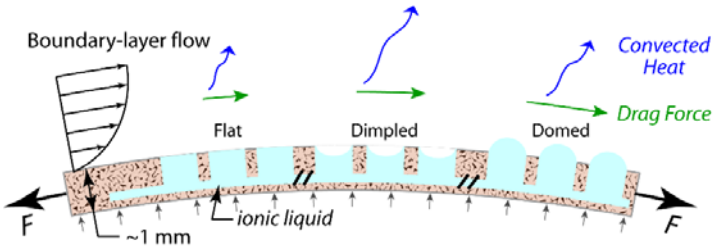

Figure 1: Notional PVC cross-section showing three menisci configurations and their effects on aerodynamic drag and heat convection.

Initial PVC designs attempted to create EWOD electroding on each pore wall near surface exits [1, 2]. However, reliably creating good quality (dielectric) coatings on every pore wall proved to be impossible, so this design was abandoned. Subsequent analysis [3, 4] led to the next design for menisci shape control, which uses just one "EWOD actuator" to control liquid pressure. The Laplace equation, described below, relates pressure differential across a liquid-air (or 2nd liquid) interface to the interface curvature and interfacial tension, and curvature can be controlled by EWOD contact angle changes. The latest PVC design consists of a laminate skin with vascular channels and pore arrays with an external EWOD actuator and displacement-pump (Figure 2-left). For research purposes, this discrete "sub-component" design is much easier to fabricate, characterize, and optimize for structural and (liquid) surface-roughness function performance. Future versions will integrate the EWOD actuator and pump with the PVC laminate (e.g., liquid-control base layer).

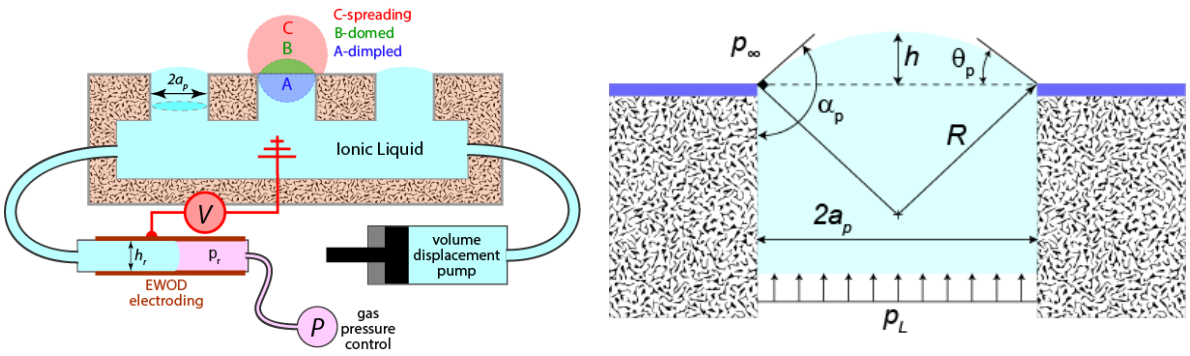

Figure 2: (Left) conceptual PVC design showing the PVC laminate, EWOD actuator, displacement pump, and fluid connections. (Right) pore cross-section showing the relevant design variables.

In EWOD, an applied voltage between a conductive liquid in contact with a hydrophobic-insulated electrode can produce apparent changes in the liquid-solid contact angle from non-wetting (> 90 deg) to wetting (< 90 deg). Benefits of EWOD liquid control compared to other liquid actuation methods include low power consumption, no moving parts, few components and simple fabrication. Initial PVC designs relied solely on EWOD actuation to control pore menisci (once the system was filled with liquid via displacement pumping), however, in order to access the full range of pore menisci shapes it became apparent that pumping was required in some situations. For example, for a system using an EWOD actuation reservoir that was closed to the atmosphere, the pore menisci contact angle control was limited to ~15-30 degrees due to the gas pressure acting against the liquid within the actuator. Analysis determined that the range of motion could be increased if EWOD actuation was supplemented with displacement pumping. In another design iteration using an EWOD reservoir that was open to the atmosphere, liquid pinning prevented complete meniscus reversibility and displacement pumping was required to recover the original meniscus shape.

The paper will start with an overview of the PVC liquid-control design showing how to size the different components to achieve the desired pore array menisci configurations. Design, fabrication, and response characterization of the EWOD actuator is covered next. Menisci control experiments using

single pore and nine-pore array PVC prototypes are described along with preliminary results on the menisci dynamics under ad-hoc boundary-layer flows. The paper will conclude with a summary of the key research findings and plans for future work.

2 PVC LIQUID-CONTROL DESIGN

There are four components that must be designed for menisci shape and height control in PVCs: the laminate skin with internal channels and pores, the EWOD actuator, a displacement pump, and the liquid connections between these components. The EWOD actuator is used to control the liquid pressure via changes in contact angle, and pressure is linked to the menisci shape via the Laplace relation. The displacement pump is used for liquid height control within the pore and to assist with menisci shape control when the liquid triple-lines are pinned at the pore exits. The operation of these two must be coordinated to avoid forcing liquid out of the pores onto the surface; in other words, changes in menisci shape require concurrent volume accommodations through pumping to avoid liquid spillage.

The pressure difference, Δp, across a liquid-gas or liquid-liquid boundary is governed by the Laplace relation [5] shown below in Eq. (1):

$$\Delta p = p_L - p_\infty = \gamma\left(\frac{1}{R_1} + \frac{1}{R_2}\right) \tag{1}$$

where p_L is the pressure in the liquid, p_∞ is the gas or liquid ambient phase pressure, γ is the interfacial tension, and R_1 and R_2 are the principle radii of curvature for the interface (positive for a convex meniscus). For circular pore menisci (Figure 2-right), $R_1 = R_2 = R$, and using trigonometric relations for a circular arc as defined in Figure 2, the following expression can be written for pressure at the pore:

$$\Delta p_p = p_L - p_\infty = \frac{-2\gamma}{a_p}\cos\alpha_p \tag{2}$$

The EWOD actuator design consists of parallel-plate electrodes of length, L_r, and width, w_r, separated by a small gap, h_r. The width of the actuator is much larger than the gap, $w_r \gg h_r$, so the Laplace relation for the pressure across the EWOD actuator is given by:

$$\Delta p_r = p_L - p_r = \frac{-2\gamma}{h_r}\cos\alpha_r \tag{3}$$

where p_r is the ambient pressure inside the EWOD reservoir. Assuming that pressure is constant in the liquid (static), p_L in Eqs. (2) and (3) can be equated, which provides the important relationship between the pore and EWOD actuator contact angles:

$$\cos\alpha_p = \frac{a_p}{h_r}\cos\alpha_r + \frac{a_p}{2\gamma}(p_\infty - p_r) \tag{4}$$

If the ambient-side of the EWOD actuator is vented, then $p_r = p_\infty$, and the last term of Eq. (4) disappears. This term can be important in SUAV applications, however, where p_∞ is the static and dynamic pressure on the airfoil during boundary-layer flow, and p_r is the "static" ambient pressure at the EWOD reservoir outlet (e.g., located inside the airfoil).

The value of α_r is controlled by the EWOD voltage through the Lippmann-Young relation [6], which can be used in Eq. (4) to give:

$$\cos\alpha_p = \frac{a_p}{h_r}\left[\cos\alpha_{r0} + \frac{\varepsilon_0\varepsilon}{2t\gamma}V^2\right] + \frac{a_p}{2\gamma}(p_\infty - p_r) \tag{5}$$

where α_{r0} is the zero-voltage contact angle of the liquid on the actuator electrode plates, $\varepsilon_0\varepsilon$ are the permittivity of free space ($8.85 \times 10^{-12}\ F/m$) and dielectric constant of the actuator coatings, respectively, t is thickness of those dielectric coatings, and V is the applied voltage between the (conductive) liquid and electrode-substrate.

Equation (5) can be used to design the liquid control components of the PVC. Pore menisci shapes from dome to flat to dimple are desired, these shapes correspond to $\alpha_p = 180, 90, 0$ degrees, respectively. There are multiple objectives and constraints that must be satisfied by the design for all pore menisci shapes. For example, it is important to keep the liquid-ambient interface in the EWOD actuator roughly centered, which requires proper spacing between the electrode plates (h_r) to make it possible to push the liquid into the actuator without the need for an applied voltage and without overflowing at the pore exits. Proper design to avoid liquid overflow at the pore exits is critical. Sharp corners at the pore exits will effectively pin the menisci edges, and a hydrophobic surface layer will help prevent liquid from spreading outside of the pore. Finally, pore domes must be kept below 180 degrees, which is the maximum pressure state and thus represents an unstable equilibrium when multiple pores are connected fluidically.

To demonstrate the use of Eq. (5) in design, consider a PVC with a desired $20 \leq \alpha_p \leq 160$ degrees of menisci control in arrays of nominal 1 mm diameter pores. Assume the EWOD actuator can achieve $65 \leq \alpha_r \leq 105$ degrees of control over a reasonable range of applied voltages, and further assume that $p_r = p_\infty$. Eq. (5) can be used to size the gap, h_r, for proper operation under the following conditions:

- EWOD actuator filling at zero voltage: select h_r such that: $\alpha_p \leq 160$ with $\alpha_r = 105$ degrees and $2a_p = 1$ mm $\rightarrow h_r \geq 0.138$ mm;
- Full range of pore menisci shapes: select h_r with $2a_p = 1$ mm such that: $\alpha_p = 160$ degrees with $\alpha_r \leq 105$ degrees and $\alpha_p = 20$ degrees with $\alpha_r \geq 65$ degrees $\rightarrow h_r \geq 0.138$ mm (same as above) and $h_r \leq 0.225$ mm.

These calculations infer that a design with $0.138 \leq h_r \leq 0.225$ mm will operate properly under the specified requirements. Further refinements are possible to account for possible pore-to-pore diameter variations (i.e., avoid liquid overflow when exceeding $\alpha_p = 160$ degrees in the largest pore), variations in EWOD substrate performance, etc. Eq. (5) can be used in similar analyses of channels and connections to assure void-free filling behavior.

The displacement pump and EWOD actuator reservoir must be able to accommodate the expected liquid volume associated with changes in menisci shape (and height) within the pore. The pore meniscus volume in going from dimple to dome equals the volume of a sphere with a diameter equal to that of the pore; so for n pores:

$$\Delta V = n\frac{4\pi}{3}a_p^3 \tag{6}$$

Assume a PVC implemented as an airfoil trip-strip that is 150 mm long by 6 mm wide with 1 mm diameter pores spaced 1 mm apart along the length and 1 mm offset between each row. Such a trip-strip would have a total of 453 pores, and the total volume change in going from dome to dimple, or vice versa, would be: 237 mm^3 or 0.237 cc. The PVC displacement-pump and EWOD actuator must be designed with a capacity of 0.24 cc or more to accommodate the expected liquid volume changes in this trip-strip.

One final design consideration will be mentioned here, and that is the speed with which changes in menisci shape and height can be made by displacement pumping without exceeding the pressure associated with pore-overflow ($\alpha_p = 160$ degrees). The pressure drop for laminar flow in a circular pipe is given by [7]:

$$\Delta \mathrm{p} = \frac{8\mu L Q}{\pi r^4} = \frac{-2\gamma}{a_p}\cos\alpha_p \tag{7}$$

where the expression on the right comes from Eq. (1), μ is the dynamic viscosity (0.001 to 0.2 N-sec/m^2, water to oil), L is the total channel length, Q is the volume flow rate, and r is the channel radius. Solving

for Q, assuming a vascular channel that spans the length of the trip-strip ($L = 0.15\ m$), and taking $r = 0.001\ m;\ \mu = 0.01\ \frac{N\ sec}{m^2};\ \gamma = 0.05 \frac{N}{m};\ a_p = 0.0005\ m;\ \alpha_p = 160\ deg$ gives:

$$\mathrm{Q} = -\frac{\pi r^4}{8\mu L} \times \frac{2\gamma}{a_p} \cos \alpha_p = 4.9\ \times 10^{-8} m^3/sec = 0.049\ cc/sec \tag{8}$$

The volume in going from dimple to dome is 0.24 cc, so Eq. (8) implies that approximately 5 seconds would be needed for this dimple to dome transition (not applicable to EWOD menisci changes). Keeping pump flow rate at less than 0.049 cc/sec will prevent the backflow pressures from exceeding that corresponding to $\alpha_p > 160\ deg$, thereby avoiding pore overflow. Similar calculations can be made for other potential restrictions in the network, and Eq. (8) can be used for component sizing to enable a desired rate-of-change in the surface roughness.

3 EWOD ACTUATOR DESIGN, FABRICATION, AND CHARACERIZATION

Previous works [1-4] have identified some design features that are necessary for effective pore meniscus control in PVCs. One is the need for a compact and robust EWOD actuator for precise control of liquid-pressure through contact angle changes. A small-gap planar design is being explored for this purpose. Two conductive silicon or glass/ITO substrates with high-quality (pin-hole free, uniform thickness) dielectric and hydrophobic coatings are bonded together and sealed around the perimeter. This creates a rectangular actuation chamber with a thickness that is much smaller than the length and width. This approach enables the use high quality EWOD substrates, but it comes with some practical challenges: 1) achieving a gas/liquid-tight seal around perimeter; 2) minimizing liquid pinning along the seal edges; and 3) integrating inlet/outlet connections that are appropriately sized and sealed.

The remainder of this section will report on recent efforts to design, fabricate, and characterize planar EWOD actuators, menisci control in single- and nine-pore PVC prototypes, and preliminary experiments examining the effects of boundary layer flow on menisci shapes and interactions.

3.1 Methods

Polished glass/ITO slides (7 Ω/sq.) and highly doped silicon wafers (0.001 Ω/sq.) were used for the EWOD substrates. Substrate specimens were first cleaned with acetone, methanol and deionized water and then treated with Silane A-174 adhesion promoter. Parylene C (5 µm-thick layer) was then deposited on the substrates using a PDS 2010 Parylene Coater from Specialty Coating Systems followed by spin-coating with Teflon AF 1600 (2% by wt. in Fluorinert FC-40; ~300 nm thick). The samples were then placed on a hot plate at 70°C for 20 min to drive-off the Fluorinert solvent. A 1:1 (v/v) mixture of 0.1 M NaCl and glycerol was used as the liquid phase for all the EWOD characterization experiments.

EWOD characterization experiments were performed on each substrate type prior to fabricating the actuators. These experiments were performed by depositing a ~5 µl drop of liquid through a 30 gauge needle onto the substrate surface and then applying either positive DC or AC (1 kHz sine wave, voltage reported is rms) voltages between the needle and the grounded substrate. The voltage was held constant while pumping liquid into and out of the drop through the needle via syringe pump. Voltage was applied with an Agilent 6612C power supply and a TREK 2050 amplifier, and droplet images were recorded every 0.5 s using Prosilica GC750 and GC1600H cameras. Advancing and receding contact angles were determined from droplet shape measurements using FTA32 software.

The resulting contact angle data (average of advancing and receding contact angles) was compared with Lippmann-Young predictions based on independently measured values for ε, t, and γ. The dielectric coating thickness, t, and coated substrate roughness were measured using a Tencor P-16 surface profiler. Surface tension, γ, of the glycerol/NaCl solution was measured using the pendant drop method and FTA32 software. Dielectric constant, ε, was measured with an Agilent E4980A LCR meter.

Fabrication of prototype EWOD actuators using a silicon substrate base and an ITO substrate top cover (for visual observation of the liquid-gas interface location) proceeded as follows. Prior to coating, a liquid inlet hole was laser cut into the glass/ITO slide. The glass/ITO and Si wafer were cleaned, and one corner of the glass/ITO slide was masked with Mylar or Kapton tape to enable an electrical connection. Both substrate types were then coated with Parylene-C. A 150 µm-thick layer of Scotch 410 M double-sided tape was then laser cut and bonded to the Parylene-coated Si wafer, forming the EWOD reservoir gap. Both substrates were then spin-coated with Teflon AF. A small area on the coated silicon substrates was scraped for the electrical connection. The silicon and glass/ITO layers were then bonded together to create a sealed chamber. Conductive paint (18% Ag) was used to make electric connections on the glass/ITO and Si wafer. An inlet port mount was created using a short length of Ø3 mm ID stainless steel tubing inserted in a poly(methyl methacrylate) (PMMA) disk. The IDs were aligned, and the mount was epoxied in-place. Relatively large fluid connections were selected to allow liquid flow into the reservoir without causing overflow at PVC pores. Figure 3 shows an exploded view of the prototype system.

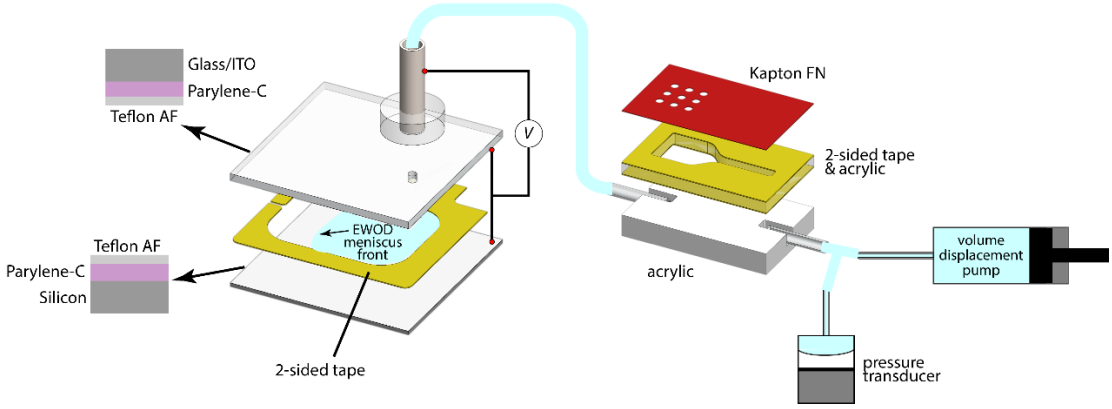

Figure 3: Schematic of the EWOD actuator, PVC pore section, pressure sensor, and syringe pump used in the experiments.

PVC (pore-channel) prototypes were fabricated for laboratory testing and demonstrations. They were laminates made with a 3 mm-thick PMMA base, a 1.5 mm-thick PMMA channel layer, and a 75 µm-thick Kapton 300FN929 pore layer (12.7/2.00/12.7 µm laminate of FEP-Kapton HN-FEP). The channel and pores were machined using a 50 W CO_2 laser cutter from Universal Laser Systems. The layers were bonded together using Scotch 410 M double-sided tape that was laser cut to match the PMMA channel layer. A sacrificial tape layer was applied to the Kapton pore layer to minimize laser cutting damage. The fluorinated ethylene propylene (FEP) layer is hydrophobic to minimize droplet spreading at the pore exits. Liquid inlets/outlets were created by bonding Ø1.1 mm ID glass capillaries into laser-cut slots in the 3 mm-thick PMMA base. The hydrophilic nature of the glass inlet/outlet tubes promoted filling. Silicone tubing (Ø1.5 mm ID) was used to connect the various components; they were flushed with methanol followed by N_2 gas to promote wetting. A KD Scientific syringe pump was used for system filling.

For EWOD actuation of the PVC, voltage was applied to the actuator reservoir metal inlet tube while the actuator substrates were grounded. Each voltage was applied for a minimum of 20 s while contact angle images were collected. The procedures used earlier for substrate EWOD characterization were again used to image and measure pore menisci characteristics. A LabVIEW program was used to sync voltage, image capture, pressure measurements, and to collect data.

3.2 Results and Discussion

EWOD response data for the silicon and glass/ITO substrate electrodes can be seen in Figure 4. As expected from the Lippmann-Young relation, the underlying substrate material has essentially no effect on EWOD, so there is little difference in response between polished silicon and glass/ITO. Voltage type

(AC or DC) likewise had little effect. The glycerol/NaCl solutions exhibited an average zero-voltage contact angle of 107° on both substrates, and the data closely followed the Lippmann-Young relation until reaching saturation (~65°; ~140 V). At saturation, the droplets exhibited an apparent stick-slip behaviour of the triple-line with continued volume increases [8].

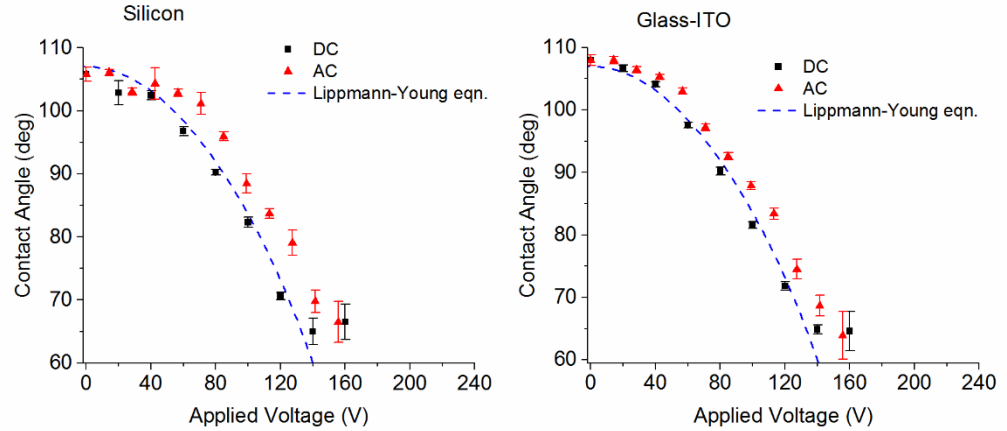

Figure 4: Contact angle vs. applied voltage (DC and AC) for a 1:1 solution of glycerol/NaCl on silicon and glass/ITO substrates. The AC voltages are V_{rms}.

Pore meniscus behaviour for a single-pore PVC can be seen in the voltage cycling data shown in Figure 5. In this plot and hereafter, the reported voltages are V_{rms}. AC voltage was incremented every 20 s from 0 V to 92 V and back to 0 V while measuring θ_p (see Figure 2-right) with no pumping (i.e., the liquid volume was held constant). Figure 5-left shows contact angle measurements and AC voltage vs. time. Profile images of the meniscus are superimposed at various voltages to visually illustrate the meniscus shape. The graph on the right shows average θ_p values for each voltage and the theoretical θ_p values calculated using Eq. 5 ($\theta_p = \alpha_p - 90°$) where $a_p = 0.5$ mm was assumed and the following parameters were measured: $h_r = 150$ µm, $\alpha_{r0} = 107°$, $\varepsilon = 3.57$, $t = 5.08$ µm, $\gamma = 0.066$ N/m, and $p_\infty = p_r$.

The pore-surface contact angle, θ_p, showed very little change from its initial 75° value until the applied voltage reached approximately 60 V, and then θ_p rapidly adjusted with each increase in AC voltage. Lack of meniscus shape change for EWOD voltages < 60 V is consistent with the EWOD substrate response data shown in Figure 4. At roughly 92 V, $\theta_p \approx 0°$, although it was not possible to directly measure this angle because the meniscus profile was not visible. Rather, the angle was inferred by observing a flat liquid surface at the pore exit by comparisons with θ_p measurements taken immediately before and after 92 V was applied. Negative θ_p (dimpled meniscus) were observed in other experiments with voltage increases above 92 V, but because the liquid profile was not visible in a side-on view at this voltage, accurate θ_p measurements were not possible. An estimate of $\theta_p \approx -50°$ was obtained using Eq. (2) with pressure data from a Setra 201 pressure transducer (± 500 Pa). On return of the applied AC voltage to 0 V, θ_p increased to approximately 45° corresponding to a contact angle hysteresis of 30°. The $\Delta\theta_p$ response and the hysteresis observed in this experiment show an improvement from previous experiments, but there is room for much improvement. The large hysteresis can be attributed to a pinning within the actuator, which could be overcome by using concurrent pumping to achieve a moving contact line. The liquid meniscus in the EWOD actuator advances towards the vent as the applied voltage increases. This increased volume in the actuator comes from the pore when total volume is held constant. So concurrent pumping is necessary if the meniscus front in the actuator cannot be held stationary.

The measured data and the theoretical curve generated from Eq. 5 (in red) have a similar trend and similar initial contact angles. Notable differences include that the measured θ_p decreases slightly less

with voltage than the theoretical curve below 60 V and the experimental data also display contact angle hysteresis, which is not accounted for in Eq. 5. The decreased response of θ_p to applied voltage, and the hysteresis may all be caused by liquid pinning at various locations. Liquid pinning at the pore, inside the channels, at the EWOD actuator inlet, and inside the actuator reservoir prevents natural liquid movement. This could allow the liquid meniscus at the pore to be artificially inflated but it also prevents the meniscus from returning to its original shape once an applied voltage is removed. Liquid pinning interactions in the PVC system are still not fully understood but they may be caused by sharp edges or dielectric charging. Additional analysis is planned.

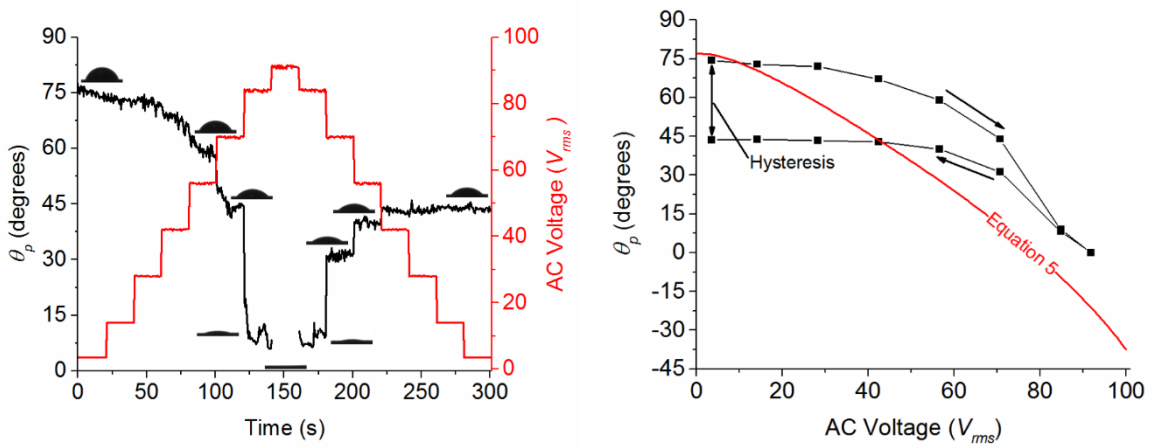

Figure 5: Single-pore PVC response to EWOD actuation at constant volume. Left: contact angle data (black with pore meniscus profiles) and applied voltages (red) vs. time. Right: average contact angle versus applied voltage. Arrows indicate time progression, and the red curve is the predicted pore contact angle from Eq. 5.

A nine-pore PVC prototype (Figure 6) connected to an EWOD actuator exhibited similar pore meniscus response as was observed with the single-pore prototype. The images in Figure 6-right were taken at four instances during the voltage cycle; the red numbers identify the corresponding voltages on the left plot. There are substantial contact angle differences between the various pores, likely due to pore-diameter and pore-wall roughness variations. The contact angle values in Figure 6 correspond to those from the pore with the largest meniscus located on the top right corner of the array.

Similar to the single-pore case, the nine-pore PVC θ_p decreased from ~75° to 4° to 40°, resulting in a ~35° contact angle hysteresis as voltage increased from 0 V to 92 V and back to 0 V. In our previously reported nine-pore PVC using the same EWOD liquid and dielectric coatings [4], θ_p decreased from 79° to 57° at 354 V_{rms} and then recovered to 73° once the voltage was removed. The improvement in menisci response with applied voltage (i.e., $\theta_p(V=0) - \theta_p(V=V_{max})$) from earlier work [4] is likely due to the smaller EWOD actuator gap (150 µm vs. 550 µm) and the use of two electroded actuator surfaces. The large hysteresis is again likely due to the lack of concurrent pumping.

One concern with the use PVC technology for active boundary-layer flow control is the possibility of menisci detachment from the pores. A simplified experiment was performed to better understand potential interactions between menisci shape and boundary-layer flow. It consisted of a nine-pore PVC subjected to a focused stream of N_2 gas flowing parallel to the PVC surface. In the top row of Figure *7*, a nine-pore PVC array is shown at different times; the yellow arrow in the left photo indicates the direction of N_2 gas flow. A second camera (View A-A) was used to observe the pore menisci profiles (Figure *7*-bottom). The pore menisci exhibited some oscillatory motion up and down during N_2 gas flow, and when the flow was varied in magnitude and direction, the liquid from a pore meniscus would sometimes detach and capture liquid from other pores it contacted as it progressed downstream. The photos in Figure 7 show a droplet detaching (lower right pore) starting at time 0 s (left). At 1.1 s, liquid from the lower right pore detached and merged with the lower middle pore. At 1.6 s, the liquid detached from the lower middle pore and carried with it liquid from the lower left pore. Finally, at 2 s, the drop

moved to the left of the pore array, and all the pore menisci had decreased their heights to accommodate the liquid volume lost from the bottom row of pores. Better understanding is needed of the pore meniscus detachment process and related physics of liquid "fracture", pore exit pinning forces, and shear force interactions during boundary layer flow. Additionally, the practical gas velocity (related to Reynold's number regime for the SUAV) must be determined to identify whether liquid detachment would occur in an operational setting.

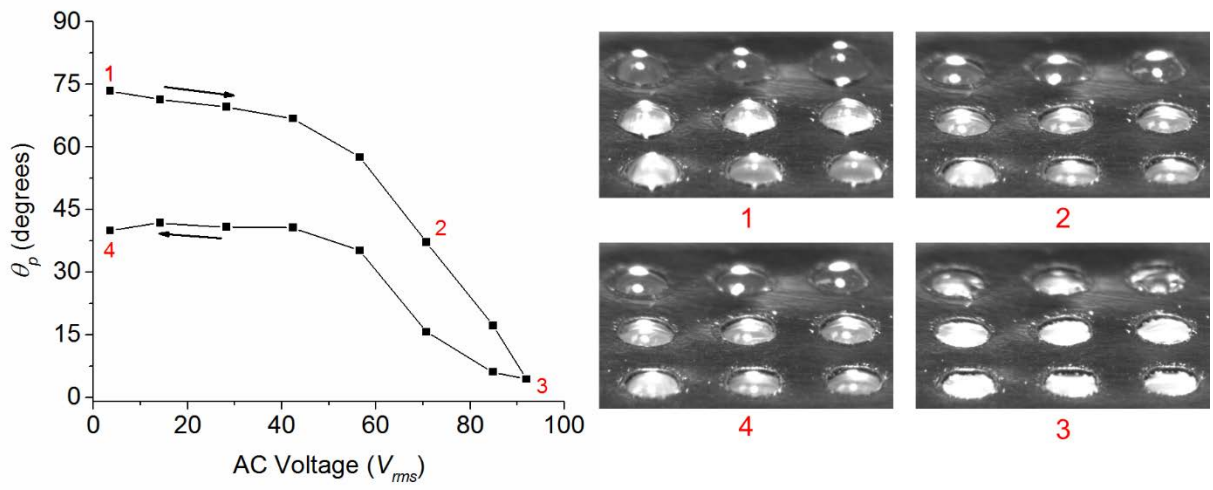

Figure 6: Nine-pore PVC contact angle vs. voltage experimental data and images showing the menisci at four points on the voltage cycle.

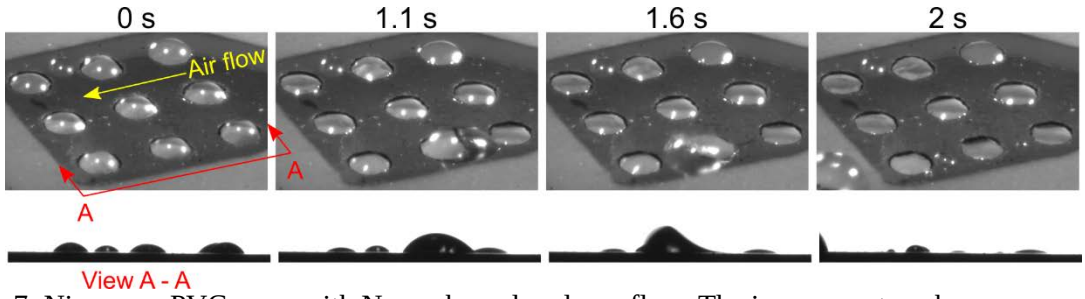

Figure 7: Nine-pore PVC array with N_2 gas boundary layer flow. The images on top show a sequence of pore liquid detachment (bottom right pore) and subsequent liquid removal from the downstream pores. The bottom images show the same event in a side-on view.

4 CONCLUSIONS AND FUTURE WORK

Recent developments in PVCs have resulted in improved surface morphology control relative to previous designs. Complete dome to dimple meniscus shapes were observed in a nine-pore PVC connected to an EWOD actuator with good-quality electrode surfaces, a decreased reservoir height (150 µm vs. 550 µm), and a large reservoir height to width ratio. PVC component analysis provided new understanding of the design rules for pore and channel dimensions, liquid flow rates, and potential liquid overflow at the pore exits. The causes of contact angle hysteresis present a continuing opportunity for scientific research that will hopefully yield new insights into the relationships between interfacial tension and electrostatic forces and their effects on liquid pinning by physical or electrical means. Technologically, concurrent pumping to enforce an advancing/receding contact angle condition within the EWOD actuator should provide a near-term solution.

On the structure-function side, research is being conducted to develop PVC laminates made from structural materials, including G-30 glass-polyimide with adequate stiffness and strength for SUAV structural applications. Experiments are being conducted on micromachining fabrication to create pores

and channels with desired liquid-control features (e.g., sharp-pore exits, machined-dimension control, channel and pore wall wetting, etc.). Pore and channel dimension and configuration effects on PVC strength and damage tolerance are also being studied. PVC materials and designs that promote liquid filling and minimize stress-concentrations are needed. The use of a hydrophobic surface layer is also being explored to prevent or minimize the propensity for liquid spillage/seeping from the pore exits.

The research has primarily been focused on developing liquid menisci shape and height control in PVCs using EWOD actuation and pumping, targeting SUAVs as a possible application. For this reason, and to make prototyping easier, pore arrays and EWOD actuators have been fabricated on the mm-scale but there is potential to move toward μm-scale components. At this scale, the surface to volume ratio increases and therefore surface tension dominates gravity and inertial effects even more than at the mm-scale. This, combined with clean room fabrication techniques for making micropore arrays and actuators with clean surfaces and very sharp edges, could result in pore menisci that are less susceptible to detachment under airflow and have less hysteresis. Such a micropore array and EWOD actuator could one day be useful in microelectronics cooling. For example, a micropore surface and micro EWOD actuator could be connected to a thermoelectric device in a microelectronics system. Using the thermoelectric output voltage as an input to the EWOD actuator could result in a smart microelectronics cooling system with improved convective heat transfer with increasing temperature. This is just one idea that illustrates the additional scientific questions and associated applications that are possible from further pursing PVC research.

5 ACKNOWLEDGEMENTS

Support for this research by Air Force Office of Scientific Research (AFOSR) under agreement number F4FGA05239G001 is very gratefully acknowledged.

6 REFERENCES

[1] J.P. Thomas, M.H. Merrill, K.M. Metkus, A. Piqué, and R.K. Everett, Multifunctional composites with applications to energy performance and efficiency, presented at the 18th International Conference on Composite Materials, Jeju, Korea, 2011.

[2] J.P. Thomas, M.H. Merrill, A. Smith, D. Kessler, M. Baur, and C. Kindle, Two-Phase Poro-Vascular Laminates with Structure-plus-Surface Roughness Control, presented at the 19th International Conference on Composite Materials, Montreal, Canada, 2013.

[3] M.H. Merrill, J.P. Thomas, R.C.Y. Auyeung, and A. Pique, Electrowetting Actuation Methods for Surface Morphology Control of Multifunctional Composites, presented at the 29th Annual Technical Conference of the American Society for Composites, La Jolla, California, 2014.

[4] J.P. Thomas, M.H. Merrill, R.C.Y. Auyeung, and A. Piqué, Poro-Vascular Composites with Surface Roughness Control, presented at the 20th International Conference on Composite Materials, Copenhagen, Denmark, 2015.

[5] P.-G.d. Gennes, F. Brochard-Wyart, and D. Quere, *Capillarity and Wetting Phenomena*. New York: Springer-Verlag, 2004.

[6] M. Frieder and B. Jean-Christophe, Electrowetting: from basics to applications, *Journal of Physics: Condensed Matter*, **17**, (2005), p. R705.

[7] B.R. Munson, D.F. Young, T.H. Tokiishi, and W.W. Huebsch, *Fundamentals of Fluid Mechanics*, 6th ed.: John Wiley & Sons, Inc., 2009.

[8] R.C. Reid, M.H. Merrill, and J.P. Thomas, Electrowetting-on-Dielectric Stick-Slip Behavior with Contact Angle Saturation, (in progress).